COMPARATIVE STUDY OF LEVELS OF RESIDUAL STRESSES OBTAINED NUMERICALLY AS A FUNCTION OF WELDING CURRENT

Pablo Batista Guimarães, pabloguimaraes@recife.ifpe.edu.br[1]
Paulo Marcelo Almeida Pedrosa, pmarcelo@hotlink.com.br[2]
Yogendra Prasad Yadava, yadava@ufpe.br[2]
Anibal Veras Siqueira Filho, anibal_siqueira@yahoo.com.br[2]
José Maria Andrade Barbosa, jmab13@gmail.com[2]
Ricardo Artur Sanguinetti Ferreira, ras@ufpe.br[2]

[1]Instituto Federal de Educação, Ciência e Tecnologia de Pernambuco, Av Professor Luiz Freire, 500, Cidade Universitária-PE, CEP 50740-540, Recife-PE.
[2]Universidade Federal de Pernambuco; Departamento de Engenharia Mecânica, Av. Ac. Hélio Ramos s/n, Cidade Universitária, CEP 50.740-530, Recife-PE.

Abstract. *The objective of this study was to define conditions for performing the welding operations to develop lower levels of residual stresses, reducing the appearance of cracks. The material used in this study was ASTM AH36 steel and welding currents used were 142A, 152A and 162A. The aspects related to the mathematical modeling of complex welding procedures were pondered with the FEM: variations in the physical and mechanical properties of the materials as a function of the temperature, the transience and the speed of the welding process, the material phase transformations, the different mechanisms of heat exchange with the environment (convection and radiation), all them associated with a high level of nonlinearity. The heat source used in this analytical model for heat supply was the double ellipsoid model proposed by Goldak, in which a 60 mm x 50 mm and 3 mm rectangular ASTM AH36 steel plate was used for the TIG process simulations. Differences were observed in the levels of residual stresses due to variation of welding current.*

Keywords*: Residual Stress, Welding Current, Steel ASTM AH36.*

1. INTRODUCTION

The multiplicity of phenomena affecting a welding process and their microstructural heterogeneity has been a complicating factor for the theoretical analysis and prediction of the physical and mechanical properties of welded joints (Tsirkas et al., 2003; Monin et al., 2000).

The resulting heterogeneous and complex microstructures followed by residual stresses cause the mechanical properties of a welded joint to be harder do forecast. Residual stress has been defined as any existing tension in the volume of a material without applying any external load (Masubuchi, 1980 and Bhadeshia 2004). The state of residual stresses is an important factor that determines the load capacity and the lifetime of a structural element. Residual stresses greatly influence the characteristics of the mechanical strength of the structural elements, considering their development after several technological processes as well as welding, thermomechanical processes, surface or thermochemical treatments, all caused by heterogeneous plastic deformation, sometimes supported by thermal action and / or phase transformations.

Studies on residual stresses have been used to define the conditions to carry out welding operations, developing lower levels of residual stresses and reducing the development of cracks. In this study, an experimental methodology was developed to numerically determine the residual stresses of a welded joint. This numerical model is based on the coupling of different physical phenomena of thermal, mechanical and metallurgical natures existing in a welding operation. In order to do that, an analytical heat source double ellipsoid model proposed by Goldak et al. (2005) was used to model the heat input. This model can be easily adopted by the industry because the input parameters of the welding process, such as electrical current, voltage and welding speed, can be controlled.

In the fusion arc welding process, the energy is concentrated in one region of the joint where the welding is being performed while the remaining material stays at lower energy regions. Under these conditions, a complex temperature field is generated as a function of both position and time producing a non-uniform and transient (time-changing) temperature distribution. Thus, the expansion of the natural hot regions is limited by the adjacent and less heated regions, generating a non-uniform plastic deformation. These heterogeneous deformations besides the cordon are responsible for much of the residual stresses produced by the welding.

According to Gurova et al. (2008) and Castello et al. (2008), another factor that may lead to the development of residual stresses are the volume changes (expansion or contraction) occurring during the phase transformations in solid. In summary, according to Macherauch et al. (1986) and Bhadeshia (2004), the development of residual stresses in welding is due to:

• Contraction during cooling in regions that are heated and plasticized differently (heterogeneous plastic deformation);
• More intense superficial cooling;
• Phase transformation;

The development of longitudinal residual stress during welding is shown in Fig. 1, where the heat-affected area (section AA') presents no temperature variations and the material remains free of tensions. Near the welding pool (section BB') the heated material tends to expand. Nevertheless, this expansion is constrained by cooler neighboring regions, so that a compressive stress is generated near ZF regions, while tensile stresses are induced in them further away. When the yield strength is reached, the heated material is plastically deformed by compression forces. In the weld pool, as the material is liquid, there is zero stress. During the solid welding metal cooling, the material begins to contract, being interrupted again by the cooler neighboring regions. These results in tensile stresses along the cord are actually strains; while in the most remote regions the stress is of compressive nature (section CC '). These tensions increase their intensity leading to the flow of heated regions. After complete cooling (section DD'), the residual stress in the welding center increases and reaches the material yield strength.

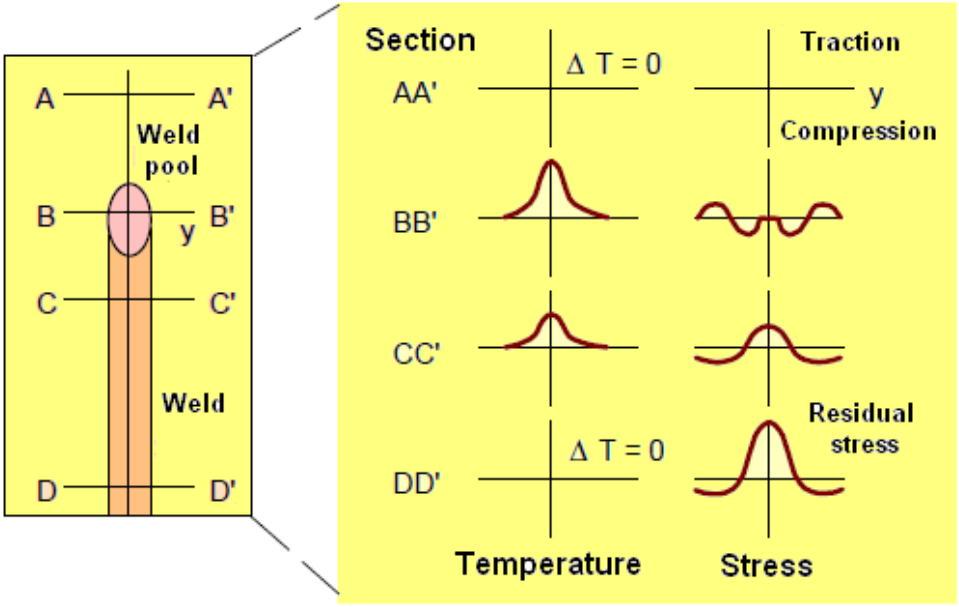

Figure 1 - Development of longitudinal residual stresses during welding (Modenesi, 2001).

Due to the intense outside cooling, a temperature gradient is established along the thickness of the piece, which combined with the temperature decline in both longitudinal and transverse directions of the cord causes residual stresses along the thickness. Residual stresses tend to increase in thicker plates due to their higher thermal gradient, considering only the faster cooling effect on the surface.

Changes in volume (expansion or contraction) occurring during the phase transformations in the solid state can also lead to the development of residual stresses. In steels, the austenite-ferrite transformation occurs with volume expansion which is hindered by the unprocessed welding bead neighboring regions (Francis et al., 2007). The intensity of residual stresses in the welding bead is related to the degree of restriction of the mechanical structure, which is usually 100% in the longitudinal direction of the weld joint.

Temperature variations in cause plastic deformations due to the thermal expansion phenomena. The deformations are accompanied by an irreversible material yield, thus resulting in a dissipation of energy in the form of heat in the material. In a numerical model this dissipative energy must be taken into account adding one more source term to the heat equation to achieve a thermo-mechanical coupling. However, a 1% plastic deformation during the loading of 400 MPa rises the temperature by approximately one degree, which can be negligible considering the welding process temperature (Danis et al., 2010; Kerrouault, 2000). The thermo-mechanical problem of the welding can be attributed to a weak coupling, in which the thermal problem that will serve as the load for the mechanical calculation will be solved in the first place. Under these conditions, the mechanical setting has no influence on the thermal field. Residual stresses can be obtained from the deformations generated during a welding process. These deformations can be either elastic (ε_{El}), plastic (ε_{Pl}), visco-elastic (ε_{VE}) or thermal (ε_{T}), so the total strain can be determined by Eq. 1.

$$\varepsilon_{Total} = \varepsilon_{El} + \varepsilon_{Pl} + \varepsilon_{VE} + \varepsilon_{T} \tag{1}$$

2. MATERIALS AND METHODS

For the simulation of residual stresses, a 60mm x 50mm and 3mm rectangular ASTM AH36 steel plate was used, considering the use of a TIG (tungsten inert gas) in the welding process. Tab. 1 shows the chemical composition of the alloy.

Table 1 - Chemical composition of the sample of ASTM AH36

C	Cr	Mn	Ni	Si	V	Al	Cu	S	P	Sn	Nb
0,130	0,026	1,418	0,012	0,346	0,056	0,028	0,015	0,007	0,023	0,002	0,020

Numerical simulations were performed with a software program (Abaqus) based on the finite element method (FEM). The board was divided into elements type DC3D8 sum to a total of 18788 elements. This mesh presented more refinement in the fusion zone and in the heat affected zone (HAZ), because those were the areas where the most important phenomena in the welding process occurred. This mesh refinement is shown in Fig. 2 and in Tab. 2.

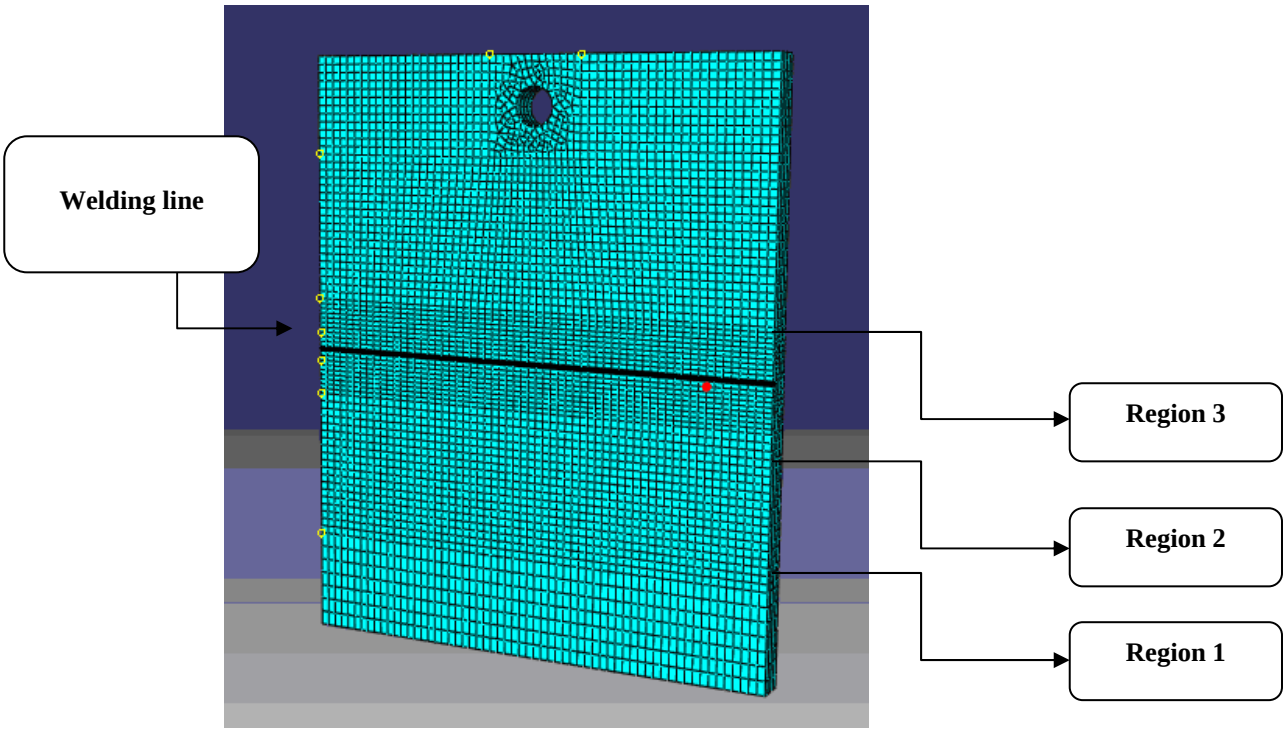

Figure 2 - Mesh and regions used for problem solving thermal and mechanical

Table 2 - Elements that make up the mesh for the FEM calculation

	Region 1	**Region 2**	**Region 3**
Number of Elements	4336	9272	4880

These elements are continuous - 3D of linear formulation and each one of them contains 8 nodes (Fig. 3). For all elements, edges along the 0,75mm thick were always used, remaining four elements along the thickness of the plate.

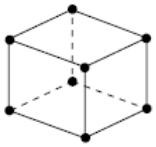

Figure 3 - Element DC3D8 - 8 nodes and linear formulation (Hibbit et al., 2007).

For the thermal boundary conditions, the exchange of convection and radiation was considered during the welding process. These boundary conditions were imported to the model. Five sides of the plate were welded, except the lower surface, which rested on the table during the welding operation. Heat exchange by convection and radiation was expressed by Eq. 2 (Newton's law) and Eq. 3 (Stefan Boltzmann's law), respectively.

$$q_c = h(T - T_0) \tag{2}$$

$$q_R = \sigma \cdot \varepsilon \cdot \left(T^4 - T_\infty^4\right) \tag{3}$$

where h is the convection coefficient, σ is the Stefan-Boltzmann's constant and ε represents emissivity. Literature values were used to model heat exchange and the assumed convection around the board. The ambient temperature considered was 25° C and emissivity 0.7. The values used for the convection coefficient (h), specific heat (C_p) and thermal conductivity (k) are shown in Fig. 4 (Tsirkas et al. 2003) as a function of temperature.

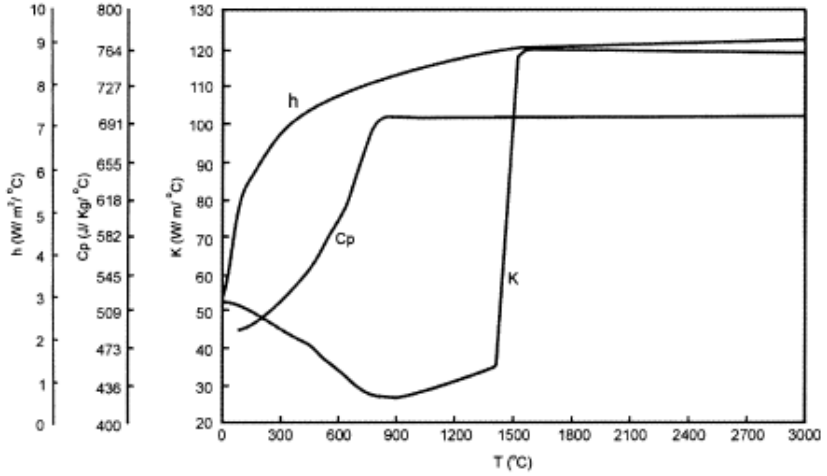

Figure 4 - Variation of material properties as a function of temperature (tsirkas et al., 2003).

The source used in this study was the double ellipsoid model proposed by Goldak, shown in Fig. 5. The geometric parameters a_f, a_r, b, c and the energy parameters f_f and f_r were obtained with the support of the relationships found in references suggested by Gery et al (2005) and Goldak et al. (2005) (Tab. 3). During the modeling, a FORTRAN DFLUX subroutine (Hibbit et al. 2007) was developed to displace the heat source. This function determines the torch position versus time, and calculates the heat input in all points of the board. Only one mechanical boundary condition was established because the plate was attached through a 4 mm diameter hole, as shown in Figure 2 (Danis et al. 2008).

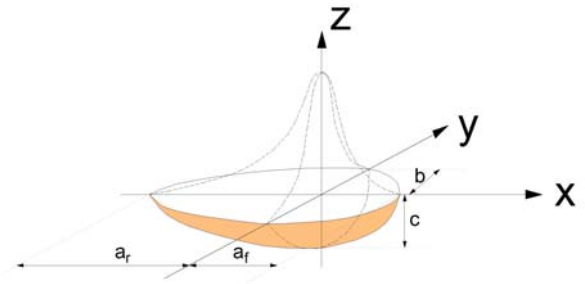

Figure 5 - Schematic representation of double source ellipsoid.

Table 3 - Geometrical parameters and energy from the heat source (Goldak & Akhlaghi, 2005, Danis, 2008).

Parameter	Value
a_f	0,0025m
a_r	0,0015m
b	0,0025m
c	0,003m
f_f	0,6
f_r	1,4

For the numerical simulations performed, in this study the value of the voltage and efficiency source were kept constant and equal to 14 V and 80% respectively. The variations in electrical current were applied. Welding parameters used in this work are shown by Tab. 4.

Table 4 - Parameters of heat input used in the numerical simulation.

Current (A)	voltage (V)	Efficiency (%)	Speed (m/s)
142	14	80	0,001
152	14	80	0,001
162	14	80	0,001

The isotropic elasto-plastic hardening was the model used to determine residual stresses, and these strains were obtained from those generated during the welding operation. These deformations were considered elastic, plastic, and thermal in nature, so the total strain was determined by Eq. 4.

$$\varepsilon_{Total} = \varepsilon_{El} + \varepsilon_{Pl} + \varepsilon_{T} \tag{4}$$

Both elastic and plastic deformations were obtained by tensile tests, and thermal deformations were obtained from the coefficient of thermal expansion as a function of temperature. Equation 5 was used.

$$\varepsilon_{T} = \alpha \cdot (T - T_0) \tag{5}$$

Considering that α is the expansion coefficient, T_0 is the room temperature and T is the temperature of a specific point, the values of the mechanical properties as a function of the temperature are shown in Fig. 6 (Tsirkas et al. 2003).

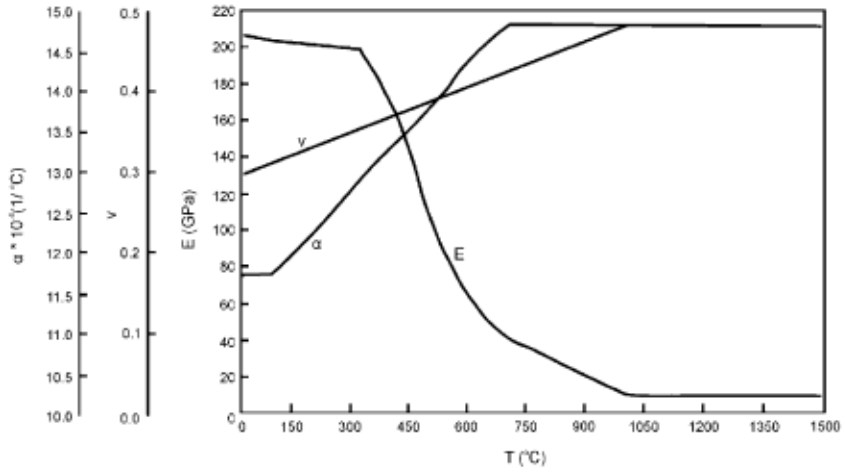

Figure 6 - Variation of mechanical properties of the material - α (thermal expansion coefficient), υ (Poisson´s ratio) and E (Young´s modulus) as a function of temperature (tsirkas et al., 2003).

The residual stress numerical model was also compared to the stress measurement method using X-Ray diffraction. A portable diffractometer was used to determine the tensions in the field. This equipment, by means of a specific software program, determines the stresses in the longitudinal directions of the welding. These stresses were determined at seven different points, as shown in Fig. 7, after the sample had been submitted to a chemical cleaning with 2% Nital solution.

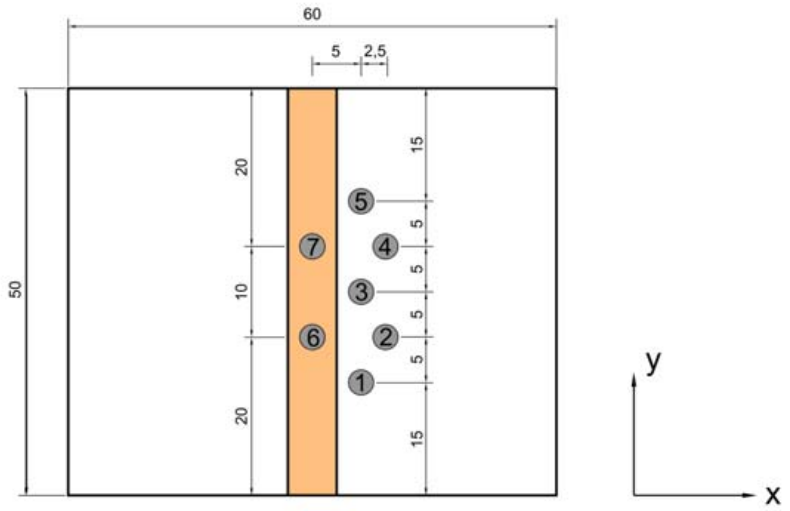

Figure 7 - Schematic representation of the points measured by X-Ray diffraction.

3. RESULTS AND DISCUSSION

Residual Stresses in the longitudinal direction to the weld after cooling plate are shown in Fig. 8 and the residual stresses in the transverse direction to the weld are shown in Fig. 9.

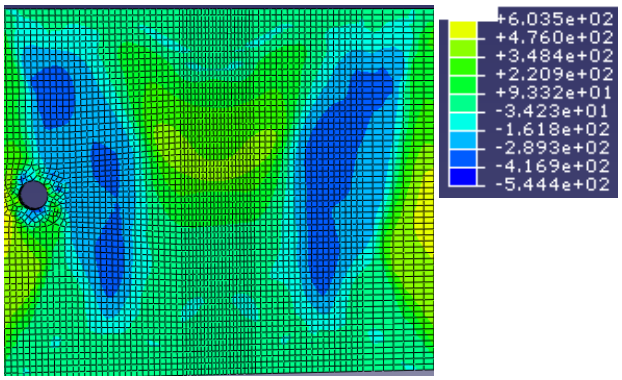

(a)

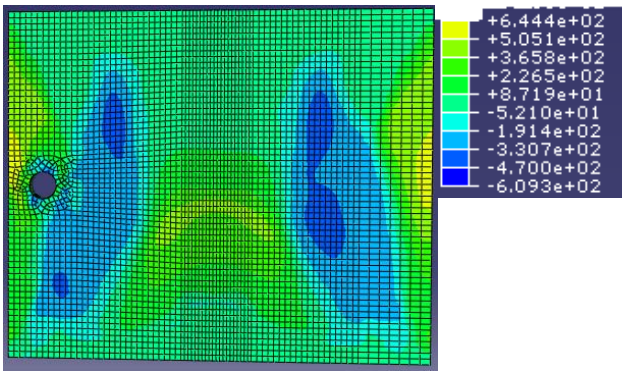

(b)

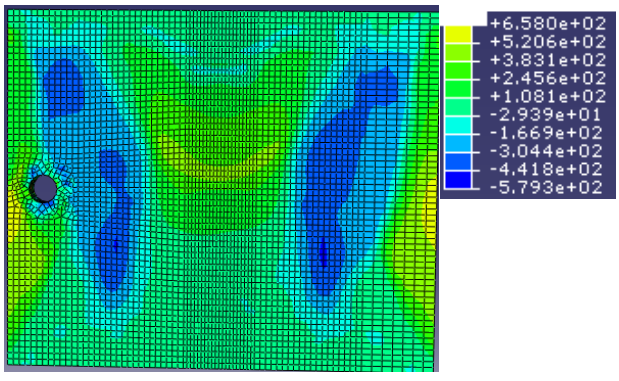

(c)

Figure 8 - Range of Residual Stresses [MPa] in the longitudinal direction for a welding current of 142A (a), 152A (b) and 162A (c).

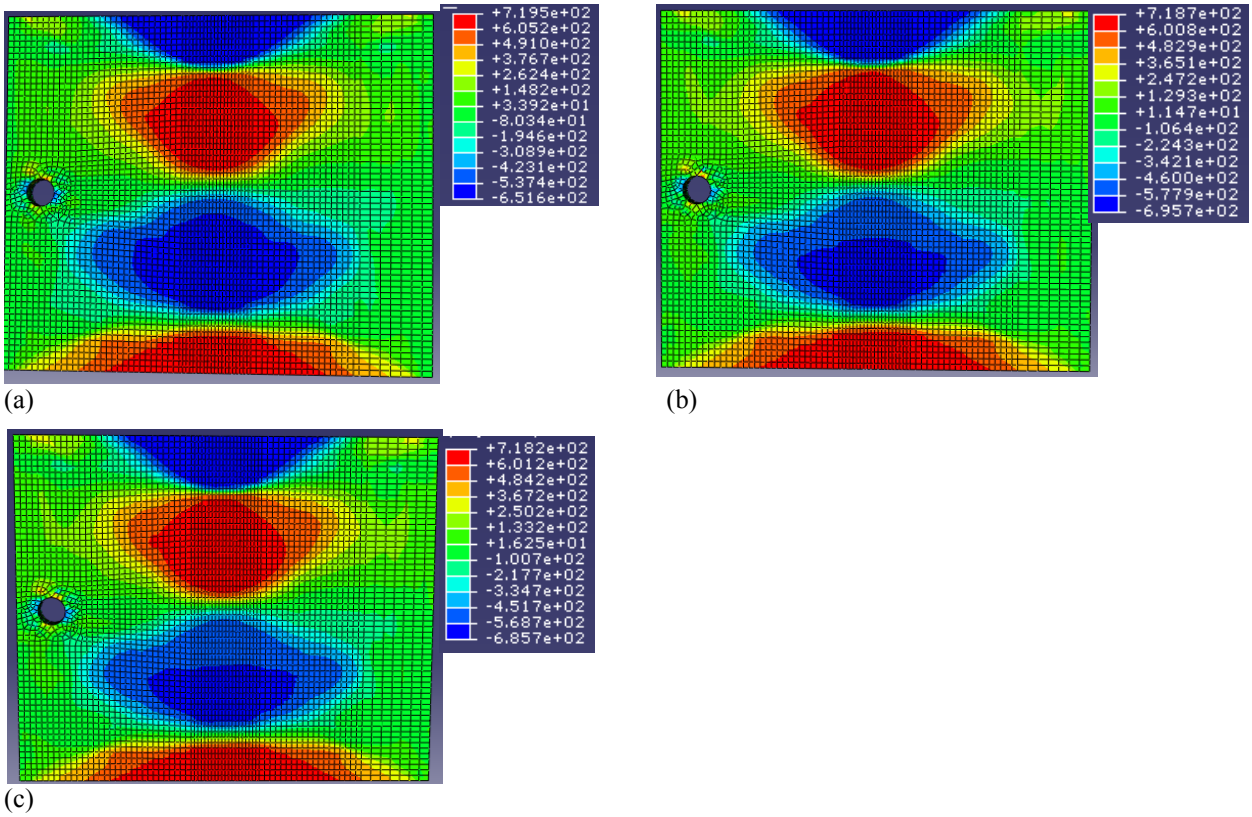

Figure 9 - Range of Residual Stresses [MPa] in the transverse direction for a welding current of 142A (a), 152A (b) and 162A (c).

Figure 10 shows the behavior of the longitudinal stresses of the welded points on seven different measurements obtained by X-Ray diffraction and by the numerical model for a welding current of 152A.

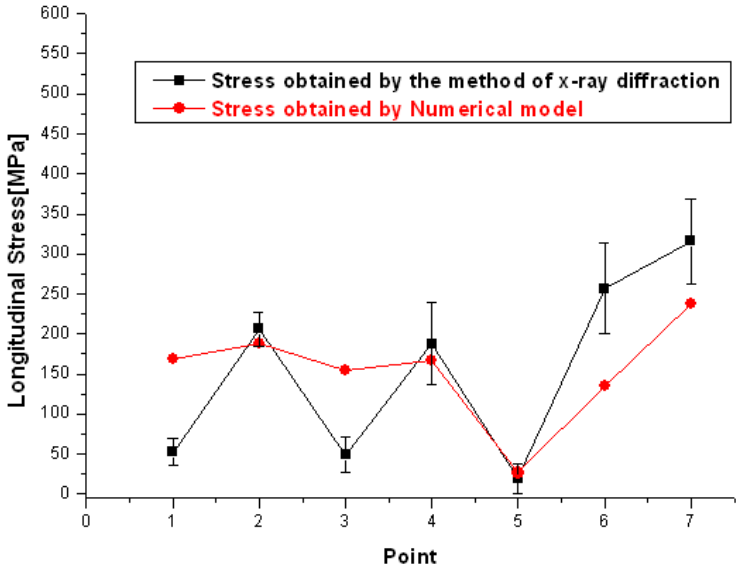

Figure 10 - Performance of residual stresses in the longitudinal obtained by the methods of X-Ray diffraction and by the numerical model for a welding current of 152A

With the cooling and solidification of the weld after the material passes to contract being prevented by colder regions and away from the weld, giving rise to tensile stresses along the cord compression and in more remote regions. As for the behavior of these strains shows this model to be consistent in terms of compressive and tractive. After cooling completely, the residual stresses in the center of the solder to reach levels of the same order of magnitude of the yield strength of the material.

The model developed with the ABAQUS software program was quite satisfactory in determining the residual stress, considering the stress measured by the X-Ray behavior, which is an established method (Monin et al. 2000; Assis et al. 2000]. The model presented higher values than those experimentally measured by X-Ray diffraction, because the welded plate recrystallized during cooling, after welding. Recrystallization is a phenomenon that is not considered by the model. In addition, it should be observed that a manual process was used; then the energy absorbed during welding was not uniform, and this had direct impact on the field under stress. The knowledge about the field where residual stresses occur in a welded joint is very important to optimize the welding procedures currently adopted in the industry, considering the reduction in the stress levels. Due to the complexity of the phenomena involved during welding, this model still needs further adjustments.

This study is just the beginning of the prediction of residual stresses, contributing to the improvement of the welding processes, particularly in establishing restrictions for the fixation of the plates during the process.

4. CONCLUSIONS

The residual stresses on the behavior of this model have shown to be consistent in terms of tractive and compressive.

After cooling completely, the residual stresses in the center of the weld reach levels of the same order of magnitude of the yield strength of the material, but still has high values in some points, requiring additional adjustments.

The determination of the temperature field in TIG welding can be simulated with ABAQUS to determine subsequent residual stresses, considering all thermo-mechanical effects. By observing phase transformation (γ–α) during virtual welding, this model presented results consistent with the practical experience.

Based on this study, it is possible to optimize a welding process by reducing residual stresses, particularly with regard to the setting of restrictions widely applied in large assembly structures in the petrochemical and shipbuilding industries.

5. ACKNOWLEDGEMENTS

We would like to thank FACEPE (Pernambuco State Foundation for Science and Technology) for their financial support to this study, as well as to the Federal University of Campina Grande for the X-Ray measurements and thanks to God.

6. REFERENCES

Assis, J. T., Monin, V.I, Pereira, F. R., 2000, "*Portable minidiffractometer for measurements in-laboratory and in-field conditions"*. 49th Denver X-ray Confer., Denver. p.219,

Bhadeshia, H.K.D.H., 2004, " *Developments in martensitic and bainitic steels: role of the shape deformation*". Materials Science and Engineering. University of Cambridge, Materials Science and Metallurgy, Cambridge, UK. pp. 34–39.

Castello, X., Gurova, T. and Estefen, S., 2008, "S*imulação das Tensões Residuais de Chapas Soldadas na Construção Naval"*. SOBENA – Sociedade Brasileira de Engenharia Naval. pp. 01-05.

Danis, P. Y., 2008, "*Étude de la soudabilité d'um superalliage base nickel fortement charge em éléments durcissants titane et aluminium: l'inconel 738*". França. 193p. (These L'Université Bordeaux 1).

Francis, J. A., Bhadeshia, H. K. D. H. and Withers, P. J., 2007, "*Welding residual stresses in ferritic power plant steels". Materials Science and Technology*. Vol. 23, pp. 1009-1020.

Gery, D., Long, H. and Maropoulos, P., 2005, "Effects of welding speed, energy input and heat source distribution on temerature variations in butt joint welding", Journal of Materials Processing Technology. Vol. 167. pp. 393–40.

Goldak, J. A. and Akhlaghi, M., 2005, "Computational Welding Mechanics", Spring - New York. pp. 30-35.

Gurova, T., Quaranta, F. and Estefen, S., 2008, "M*onitoramento do Estado de Tensões Residuais Durante a Fabricação de Navios"*. SOBENA – Sociedade Brasileira de Engenharia Naval. pp. 01-09.

Hibbit, Karlsson & Sorenson Inc., 2007, "Abaqus *User Subroutines Reference Manual* - Version 6.7", USA. "DFLUX" Section 1.1.3, "USDFLD" Section 1.1.40.

Hibbit, Karlsson & Sorenson Inc., 2007, "*Abaqus Getting Started with Abaqus* – Interactive Edition" *Versão* 6.7. USA. Section 1-4;8-10.

Kerrouault., 2000, "*Fissuration à Chaud en Soudage d'un acier inoxydable austénitique*". PhD Thesis, Centrale Paris.
Masubuchi, K., 1980, "*Analysis of Welded Structures. Residual Stress and Distortion and Their Consequences"*. Pergamon Press, Oxford-New York. pp. 33.
Modenesi, P. J., 2001, "*Efeitos Mecânicos do Ciclo Térmico"*. UFMG - Universidade Federal de Minas Gerais, 5 Mai 2008, <www.demet.ufmg.br/grad/disciplinas/emt019/tensao_residual.pdf. >.
Monin, V.I., Teodosio, J.R., Gurova, T., 2000, "*A portable X-ray apparatus for both stress measurements and phase analysis under field conditions"*. Advances in X-ray Analysis, Vol.43. p.66-71
Tsirkas, S. A., Papanikos, P. and Kermanidis, T.H., 2003, "Numerical Simulation of the Laser Welding Process in butt-joint specimens", Journal of Materials Processing Technology. Vol. 134. pp. 59–69.

7. RESPONSIBILITY NOTICE

The following text, properly adapted to the number of authors, must be included in the last section of the paper: The authors are the only responsible for the printed material included in this paper.